

Saturation behavior of two x-ray lasing transitions in Ni-like Dy

R. Smith,¹ G. J. Tallents,¹ J. Zhang,² G. Eker,¹ S. McCabe,³
G. J. Pert,³ and E. Wolfrum²

¹*Department of Physics, University of Essex, Colchester CO4 3SQ, United Kingdom*

²*Department of Physics, Clarendon Laboratory, University of Oxford, Oxford OX1 3PU, United Kingdom*

³*Department of Physics, University of York, York YO1 5DD, United Kingdom*

(Received 17 August 1998)

Saturated operation of a laser at a wavelength shorter than 6 nm is demonstrated. The output of the Ni-like Dy laser at 5.86 and 6.37 nm, pumped by the VULCAN 1.05- μm Nd-glass laser in a 75-ps double-pulse configuration at $2 \times 10^{13} \text{ W cm}^{-2}$ peak irradiance, is measured experimentally and studied theoretically using a rate equation and one-dimensional amplified spontaneous-emission model. The experimental results and modeling show that, upon saturation, the output intensities from the lower gain lasing transition at 6.37 nm decrease with increasing gain medium length. This is a different signature of gain saturation for Ni-like lasers and is desirable for applications, as it shows that one lasing transition will dominate with Ni-like lasers in saturation. [S1050-2947(99)50901-3]

PACS number(s): 42.55.Vc, 42.55.Ah

One of the important goals for laser research is to achieve saturated operation of x-ray lasers in the “water window” wavelength range of 2.2–4.3 nm [1]. Saturation of a gain medium occurs when stimulated emission becomes a significant depopulating process on the upper quantum-state population. Saturated operation of an x-ray laser is desirable because it means that the maximum power possible for a given volume of excited plasma is extracted by stimulated emission, and an output sufficiently intense for applications is produced with little shot-to-shot variation. Saturation of x-ray lasers is usually diagnosed by measuring the laser output as a function of lasing medium length [2] and by measuring the absolute output irradiance for comparison to calculated saturation irradiances [3]. Confirmation of saturation can be seen by making the difficult measurement of the lasing line spectral width to monitor gain narrowing [4].

The Ni-like lasers exhibit gain on two $J=0-1$ transitions emanating from the same upper quantum state. In this paper, we report an observation of saturated operation for the Ni-like Dy x-ray laser at 5.86 and 6.37 nm, and describe how the saturation behavior of the two lasing transitions can act as a signature for saturation in Ni-like x-ray lasers. Ni-like Sm at 7.36 nm was the shortest saturated laser wavelength previously reported [2]. An equation for saturated gain is found from a rate equation model and by integrating along the gain medium length; an expression is found for the variation of the output lasing intensity for the two transitions. We show that experimentally measured laser output for the Ni-like Dy transitions at 5.86- and 6.37-nm wavelengths is well reproduced by the simple modeling if we allow the small signal gain coefficients as fitting parameters. Atomic physics modeling [5] shows that the gains for the two $J=0-1$ lasing transitions for Ni-like ions are close to equal for Gd with atomic number $Z \approx 64$, but become increasingly unequal for both lower and higher Z with increasing distance of Z away from 64. As Ni-like lasers of high Z are developed with lasing at shorter wavelengths, it should be relatively straightforward to monitor the output intensity, as a function of gain medium length, of the lower gain transition as a check of saturation.

Six beams from the VULCAN 1.06- μm Nd-glass laser with pulse widths of 75 ps were employed in a standard off-axis line focus geometry [6] to irradiate Dy stripe targets. The targets were pumped using a double-pulse configuration in which a prepulse, with 10–20% of the total energy, was incident on target 2.2 ns before the main pulse. The prepulse generates a preplasma that reduces the density gradients in the direction away from the target surface. This allows for more efficient energy coupling from the main pumping pulse and also serves to reduce refraction effects, which can deflect x-ray photons prematurely out of the gain region. Three beams were focused by $f/2.5$ off-axis spherical lenses onto each target plane in a 20-mm-length line focus with a width of 100 μm . After taking into account energy losses, this arrangement delivered intensities of $\sim 2 \times 10^{13} \text{ W cm}^{-2}$ on target. The stripe targets were of length 18 mm and were set 180° opposed to each other with 150–175- μm separation between the target surfaces. X-ray laser coupling efficiencies of 50–80% between the two targets are obtained [2,7].

The time-integrated output of the x-ray laser was measured using an axial flat-field spectrometer. Gold reflection filters and an aluminum foil filter were used to spectrally isolate the Ni-like lasing lines at 5.86 and 6.37 nm. The spectrometer aberration-corrected concave grating (average line spacing of 1200 lines/mm) at 3° grazing angle incidence imaged the x-ray laser onto the detection plane. An x-ray charge-coupled-device camera was placed at the focal plane of the grating to record the intensity of the x-ray laser transitions. The x-ray laser output was recorded for a number of gain medium lengths by varying the lengths of the target materials irradiated. For lengths below 18 mm, only single targets were used. Once saturation has been achieved, Ni-like x-ray laser outputs are consistent to within a factor of 2 from shot to shot [2,7] for the same target length and typical range of pumping laser energies ($\pm 10\%$).

A reduction of the lower gain coefficient line intensity for Ni-like Dy with increasing gain medium length has been observed (Fig. 1). When the high-gain 5.86-nm line reaches saturation, the lower-gain 6.37-nm line also stops increasing

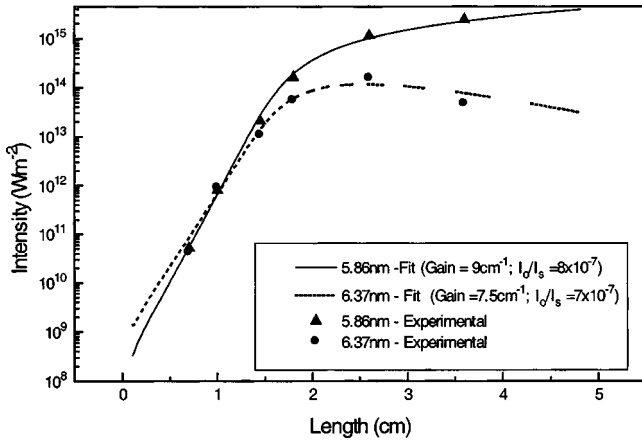


FIG. 1. Plot of the output intensity of the $4d-4p$ $J=0-1$ lasing lines for the Ni-like Dy x-ray laser as a function of plasma length. The experimental points are shown by the triangle and circle data points for the 5.86- and 6.37-nm lasing lines, respectively. The lines represent the fit from the double line saturation model with the plasma conditions represented in Fig. 3 and gains of 9 and 7.5 cm^{-1} .

in intensity with increasing length of the gain medium. In the saturation regime, the intensity of the high gain transition still increases linearly as a function of plasma length and this depopulates the common upper quantum state for the two lines through stimulated emission, causing a reduction in output for the 6.37-nm line with increasing gain medium length.

Using the labeling of Fig. 2, the steady-state rate equations for the three levels involved in Ni-like x-ray lasing can be written as

$$R_1 = N_1 \left(\frac{\mathcal{P}_3 \sigma_{31} \bar{I}_{31}}{h\nu_{31}} + A_{10} \right) - N_3 \left(\frac{\sigma_{31} \bar{I}_{31}}{h\nu_{31}} + A_{31} \right), \quad (1)$$

$$R_2 = N_2 \left(\frac{\mathcal{P}_2 \sigma_{32} \bar{I}_{32}}{h\nu_{32}} + A_{20} \right) - N_3 \left(\frac{\sigma_{32} \bar{I}_{32}}{h\nu_{32}} + A_{32} \right), \quad (2)$$

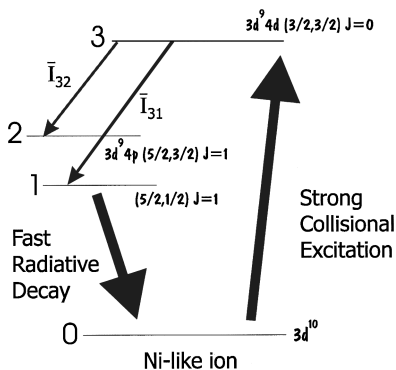


FIG. 2. Simplified energy-level diagram for a Ni-like ion. The ground state is labeled 0, the upper $4p$ lasing level is labeled 3, and the lower $3d$ lasing levels are labeled 1 and 2.

$$R_3 = N_3 \left(\frac{\sigma_{31} \bar{I}_{31}}{h\nu_{31}} + \frac{\sigma_{32} \bar{I}_{32}}{h\nu_{32}} + A_3 \right) - N_1 \left(\frac{\mathcal{P}_3 \sigma_{31} \bar{I}_{31}}{h\nu_{31}} \right) - N_2 \left(\frac{\mathcal{P}_2 \sigma_{32} \bar{I}_{32}}{h\nu_{32}} \right), \quad (3)$$

where R_1 , R_2 , and R_3 are the pumping rates into the excited quantum states; N_1 , N_2 , and N_3 represent the populations of the respective energy levels; σ_{ul} is the stimulated emission cross section between level u and l ; \mathcal{P}_1 , \mathcal{P}_2 , and \mathcal{P}_3 are the statistical weights for the levels; A_{ul} is the spontaneous decay rate from level u to l ; and $h\nu_{ul}$ is the transition energy between levels u and l . We write $A_3 = A_{30} + A_{31} + A_{32}$.

The intensity \bar{I}_{ul} for a given lasing line integrated over the emission profile $f(\nu)$ is given by

$$\bar{I}_{ul} = \frac{1}{f(0)} \int I(\nu) f(\nu) d\nu, \quad (4)$$

where $I(\nu)$ is the intensity at frequency ν ; $f(\nu)$ and $f(0)$ are the line-shape factors at frequency ν and line center, respectively.

The local gains for the two x-ray lasing transitions are given by

$$G_{31} = \sigma_{31} \mathcal{P}_3 \left(\frac{N_3}{\mathcal{P}_3} - \frac{N_1}{\mathcal{P}_1} \right), \quad (5)$$

$$G_{32} = \sigma_{32} \mathcal{P}_2 \left(\frac{N_3}{\mathcal{P}_2} - \frac{N_2}{\mathcal{P}_2} \right), \quad (6)$$

which upon simultaneously solving Eqs. (1)–(3) and neglecting nonsignificant terms, can be written as

$$G_{31} = \frac{g_{31}}{1 + \left(\frac{\bar{I}_{31}}{I_{S1}} + \frac{\bar{I}_{32}}{I_{S2}} \right)}, \quad (7)$$

$$G_{32} = \frac{g_{32}}{1 + \left(\frac{\bar{I}_{31}}{I_{S1}} + \frac{\bar{I}_{32}}{I_{S2}} \right)}, \quad (8)$$

where the saturation intensities obtained for the two lasing transitions are

$$I_{S1} = \frac{(A_{30} + A_{31} + A_{32}) A_{10} h\nu_1}{\left(A_{10} + \frac{\mathcal{P}_3}{\mathcal{P}_1} (A_{30} + A_{32}) \right) \sigma_{31}}, \quad (9)$$

$$I_{S2} = \frac{(A_{30} + A_{31} + A_{32}) A_{20} h\nu_2}{\left(A_{20} + \frac{\mathcal{P}_2}{\mathcal{P}_2} (A_{30} + A_{31}) \right) \sigma_{32}}, \quad (10)$$

and g_{31} , g_{32} are the respective small signal gain coefficients. Experimentally measured values of G_{31} and G_{32} are spatial

averages of the gain (see further discussion below), so while we will use Eqs. (7)–(10) to explain experimental observations, the values of small signal gain (g_{31} and g_{32}) will be determined by fits to the experimental data and not from Eqs. (5) and (6).

Following Pert [10], the expression for intensity integrated over the line profile necessary to calculate the reduction in the output gain due to saturation is given as

$$\bar{I} = I_0 \beta(Gl), \quad (11)$$

where

$$\beta(Gl) = \int_{-\infty}^{\infty} \{\exp[Gl\phi(v)] - 1\} f(v) dv = \frac{d\alpha(Gl)}{d(Gl)} - 1, \quad (12)$$

where $\phi(v) = f(v)/f(\phi)$ and I_0 is the ratio of the spontaneous emissivity to the small signal gain. The subscripts G_{31} and G_{32} are dropped as the equations apply to both transitions. The parameter $\alpha(Gl)$ takes into account wavelength integration over an assumed Gaussian profile and is given by the Linford approximation [11] as

$$\alpha(Gl) = \frac{(e^{Gl} - 1)^{3/2}}{(Gle^{Gl})^{1/2}}. \quad (13)$$

Expanding on the analysis of Pert [10] for amplified spontaneous emission (ASE) lasing, for two lasing transitions with a common upper quantum state, the gain length product Gl for each transition obeys the differential equation,

$$\frac{d(Gl)}{d(gl)} = \frac{G}{g} = \frac{1}{1 + \frac{\bar{I}_{31}}{I_{S1}} + \frac{\bar{I}_{32}}{I_{S2}}}. \quad (14)$$

By assuming that I_{S1} , I_{S2} , I_{O1} , I_{O2} , and g are constant along the plasma length, we may combine Eqs. (11), (12), and (14) to establish a relationship between gain and the length of the gain region for both transitions as follows:

$$g_{31}l = \left(1 - 2\frac{I_{O1}}{I_{S1}}\right) G_{31}l - 2\frac{I_{O2}}{I_{S2}} G_{32}l + 2\frac{I_{O1}}{I_{S1}} \alpha(G_{31}l) + 2\frac{I_{O2}}{I_{S2}} \alpha(G_{32}l), \quad (15)$$

$$g_{32}l = \left(1 - 2\frac{I_{O2}}{I_{S2}}\right) G_{32}l - 2\frac{I_{O1}}{I_{S1}} G_{31}l + 2\frac{I_{O1}}{I_{S1}} \alpha(G_{31}l) + 2\frac{I_{O2}}{I_{S2}} \alpha(G_{32}l). \quad (16)$$

The ratio I_0 for each transition is given by

$$I_{O1} = \frac{A_{31}}{\sigma_{31}} \frac{\Omega}{4\pi} hv, \quad (17)$$

$$I_{O2} = \frac{A_{32}}{\sigma_{32}} \frac{\Omega}{4\pi} hv, \quad (18)$$

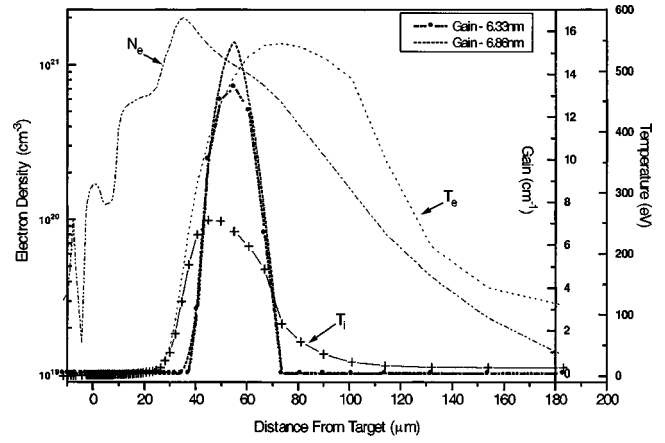


FIG. 3. Temperature and density profiles from the EHYBRID hydrodynamic and atomic physics code at the time of the peak of the main pumping pulse for the Ni-like Gd x-ray laser. Gain coefficients as a function of distance from the target are also shown for the two $4d-4p$ $J=0-1$ lasing transitions.

where Ω is the solid angle into which the spontaneous emission is amplified. The output x-ray laser irradiance I_l is given by

$$I_{l1} = I_{O1} \alpha(G_{31}l), \quad (19)$$

$$I_{l2} = I_{O2} \alpha(G_{32}l). \quad (20)$$

Through a combination of Eqs. (15)–(20), it is possible to plot the intensity of the two lasing lines as a function of plasma length (Fig. 1).

Numerical simulation of the Ni-like gadolinium x-ray laser using the 1.5-D hydrodynamic and atomic physics code EHYBRID [8] gives output profiles of the electron and ion temperatures, electron density, and the gain profiles of the two $4d-4p$ $J=0-1$ lasing transitions, as a function of distance away from the target surface (Fig. 3). The input parameters for this simulation are set to model the present experimental conditions. Taking the predicted values for the plasma conditions at the position of peak gain and by using the atomic data from Daido *et al.* [5], we may calculate the values for the saturation intensities I_S using Eqs. (9) and (10) and I_0 values using Eqs. (17) and (18) for the two lasing lines of Ni-like Dy by assuming that the plasma conditions for lasing with Gd ($Z=64$) and Dy ($Z=66$) are similar. We assume that the solid angle Ω into which spontaneous emission is amplified is given by the laser output area divided by the square of a target length of 1.8 cm. The output area has been measured at approximately $150\ \mu\text{m} \times 300\ \mu\text{m}$ for similar lasers by imaging the laser output with a multilayer mirror [9]. We obtain $I_0/I_S = 8 \times 10^{-7}$ for the higher gain 5.86-nm transition and $I_0/I_S = 7 \times 10^{-7}$ for the lower gain 6.37-nm transition, assuming Doppler broadening for the evaluation of σ_{31} and σ_{32} with an ion temperature of 250 eV. The EHYBRID calculated gains are effectively spatially averaged by the propagating x-ray laser beams. Spatial averaging of the gain occurs as refraction causes the propagating x-ray laser rays to move away from the target surface. A typical ray will traverse the gain profile shown in Fig. 3 from short to long distances from the target surface as it travels along the target length. Consequently, we have adjusted the small

signal gain coefficient assumed for the model [Eqs. (15)–(20)] to fit the experimental data (Fig. 1). The best-fit values are 9 and 7.5 cm^{-1} for the 5.86- and 6.37-nm lines, respectively. Such gains are consistent with the gain profiles peaking at 15 and 13 cm^{-1} for Gd (Fig. 3) after allowance for spatial averaging.

The ASE model developed in this paper predicts a drop in intensity for the lower gain transition with the onset of saturation for the higher gain line, in approximate agreement with the experimental results. The experimental intensity of the lower gain line in the saturation regime is up to approximately two orders of magnitude less than the higher gain line intensity, while below saturation the two line intensities are comparable. Such a relative intensity decrease is much greater than the maximum shot-to-shot variation of saturated x-ray laser intensities (\sim a factor of 2) seen in experiments with Ni-like lines [2,7]. The experimental results and model illustrate that a reduction in the gain coefficient with increasing gain medium length for the low gain $4d-4p \ J=0-1$ lasing transition is symptomatic of the high gain transition operating within the saturation regime.

To summarize and conclude, saturated lasing has been observed at wavelengths below 6 nm with the Ni-like Dy x-ray laser. The output dependence of a two-transition amplified spontaneous emission x-ray laser with gain medium length was characterized by a simple rate equation and one-

dimensional ASE model. Using these general expressions, a relationship between the gain and the length of the gain medium was found, and through integration along the plasma length the output intensities of the two transitions were calculated. Coupling these results with simulated plasma conditions and using the small signal gain coefficient as a fitting parameter, the predicted x-ray laser output as a function of plasma length was found for the two $4d-4p \ J=0-1$ lasing lines, in agreement with experimental data. It was observed both experimentally and from the model that, as a consequence of the higher gain transition saturating, the lower gain line experiences a reduction in gain coefficient. This is due to the increased depopulation rate of the common upper lasing level by stimulated transitions caused by the saturated high gain line. We have shown that the experimental observation of gain reduction for the low gain transition in the Ni-like x-ray laser is a signature that the higher gain line is operating within the saturation regime. The production of a single gain line is needed for many applications [12], and this reduction of the lower gain line output is a desirable feature for such applications.

We would like to acknowledge the contribution to this work from the staff at the Central Laser Facility and members of the U.K. X-ray Laser Consortium. The work was financially supported by grants from the U.K. Engineering and Physical Sciences Research Council.

-
- [1] J. Trebes, J. Brase, J. Gray, R. London, D. Matthews, D. Peters, D. Pikel, G. Stone, M. Rosen, and T. Yorkey, *Inst. Phys. Conf. Ser.* **116**, 279 (1991).
 - [2] J. Zhang, A. G. MacPhee, J. Lin, E. Wolfrum, R. Smith, C. Danson, M. H. Key, D. Neely, J. Nilsen, G. J. Pert, G. J. Tallents, and J. S. Wark, *Science* **276**, 1097 (1997).
 - [3] J. Zhang, P. J. Warwick, E. Wolfrum, M. H. Key, C. Danson, A. Demir, S. Healy, D. H. Kalantar, N. S. Kim, C. L. S. Lewis, J. Lin, A. G. MacPhee, D. Neely, J. Nilsen, G. J. Pert, R. Smith, G. J. Tallents, and J. S. Wark, *Phys. Rev. A* **54**, R4653 (1996).
 - [4] J. A. Koch, B. J. MacGowan, L. B. DaSilva, D. L. Matthews, J. H. Underwood, P. J. Batson, and S. Mrowka, *Phys. Rev. Lett.* **68**, 3291 (1992).
 - [5] H. Daido, S. Ninomiya, T. Imani, Y. Okaichi, M. Takagi, R. Kodama, H. Takabe, Y. Kato, F. Koike, J. Nilsen, and K. Murai, *Int. J. Mod. Phys. B* **11**, 945 (1997).
 - [6] C. L. S. Lewis, D. Neely, D. M. O'Neill, J. O. Uhomoibhi, M. H. Key, Y. Al Hadithi, G. J. Tallents, and S. A. Ramsden, *Opt. Commun.* **91**, 71 (1992).
 - [7] J. Zhang, A. G. MacPhee, J. Nilsen, J. Lin, T. W. Barbee, Jr., C. Danson, M. H. Key, C. L. S. Lewis, D. Neely, R. M. N. O'Rourke, G. J. Pert, R. Smith, G. J. Tallents, J. S. Wark, and E. Wolfrum, *Phys. Rev. Lett.* **78**, 3856 (1997).
 - [8] P. B. Holden, S. B. Healy, M. T. M. Lightbody, G. J. Pert, J. A. Plowes, A. E. Kingston, E. Robertson, C. L. S. Lewis, and D. Neely, *J. Phys. B* **27**, 341 (1994).
 - [9] J. Nilsen, J. Zhang, A. G. MacPhee, J. Lin, T. W. Barbee, C. Danson, L. B. DaSilva, M. Key, C. L. S. Lewis, D. Neely, R. M. N. O'Rourke, G. J. Pert, R. Smith, G. J. Tallents, J. S. Wark, and E. Wolfrum, *Phys. Rev. A* **56**, 3161 (1997).
 - [10] G. J. Pert, *J. Opt. Soc. Am. B* **11**, 1425 (1994).
 - [11] G. J. Linford, E. P. Poessini, W. R. Sooy, and M. L. Spaeth, *Appl. Opt.* **13**, 379 (1974).
 - [12] D. H. Kalantar, L. B. DaSilva, S. G. Glendinning, B. A. Remington, F. Weber, S. V. Weber, M. H. Key, N. S. Kim, D. Neely, E. Wolfrum, J. Zhang, J. S. Wark, A. Demir, J. Lin, R. Smith, G. J. Tallents, C. L. S. Lewis, A. MacPhee, J. Warwick, and J. P. Knauer, *Rev. Sci. Instrum.* **68**, 802 (1997).